Blade Imbalance Fault Diagnosis of DFIG based on Current Park's Transformation

Dong Yang, Xiaojun Han, Xiaowei Fu, Jianbo Du, Gang Chen, Yuanhe Gao, Jing Wang
Beijing Institute of Spacecraft System Engineering
Beijing, China
htyangdong@126.com

Abstract—**Aiming at the impeller imbalance fault of the Doubly fed Induction Generator (DFIG), a fault characteristic extraction method based on stator current is proposed. Firstly, based on the model of DFIG and its drive chain, the expression of the DFIG impeller imbalance stator current is derived. Secondly, the three-phase current of the stator is processed by Park's Transformation. Then through spectrum analyzing the squared signal of the stator current vector, the fault can be diagnosed by observing the amplitude variation of the feature frequency in the squared signal. Finally, a DFIG simulation model of is established. The fault characteristics of impeller imbalance fault at different wind speeds are analyzed by the proposed method. The results indicate that the proposed impeller imbalance fault diagnosis method in this paper can effectively extract the fault.**

Keywords-Wind Turbie; Impeller Imbalance; Staor current; Fault diagnosis

I. INTRODUCTION

With the energy crisis and environmental pollution, wind power is receiving more and more attention. In recent years, DFIG have become mainstream model. The safe and stable operation of wind turbines have attracted people's attention with the operation of a large number of wind turbines. During the operation of wind turbine, various faults are prone to occur affected by aerodynamics and harsh environment [1]. Impeller icing or pitch angle misoperation will cause impeller imbalance [2].

Vibration signal spectrum analysis method was used to diagnose impeller imbalance fault in ref [3]. The spectrum analysis method of the wind turbine shaft torque signal was proposed to diagnose the impeller imbalance fault. [5]. In the ref [4], the generator electric power the was proposed to diagnose the impeller failure of the wind turbine. Some scholars have adopted methods such as temperature, X-ray imaging and ultrasonic [6]. However, these methods have some shortcomings. For example, vibration signal acquisition requires the installation of an additional vibration sensor. Torque sensor is required for shaft torque measurement. Measuring power requires simultaneous sampling of the stator three-phase voltage and current. And, the calculation is large. It is a cost advantage to analyze the existing collected electrical signals to achieve state monitoring of wind turbine, that is the development trend of wind turbine condition monitoring in the future.

To diagnose impeller imbalance fault of DFIG, a fault feature extraction method based on stator current is proposed. Firstly, based on the DFIG and its drive chain model, the expression of DFIG stator current under impeller imbalance is derived. Then a feature extraction method based on Park's Transformation and spectrum analyzing the squared signal is proposed. Finally, by establishing simulation model of the DFIG, the stator current under different wind speeds and unbalance rates were analyzed and compared with different method. The validity of the proposed method is verified.

II. THE EFFCT OF IMPELLER IMBALANCE FAULT ON GENERATOR STATOR CURRENT

When the angular velocity is ω_{m}, the shaft torque of DFIG which is under impeller imbalance is:

$$T = T_0 + T_v \sin(\omega_m t + \varphi) \ , \tag{1}$$

Where T is output shaft torque; T_0 is aerodynamic torque; T_v is the amplitude of the torque ripple caused by the impeller imbalance.

The equation of wind turbine transmission model is [7]:

$$2H_M \frac{d\omega_m}{dt} = T - T_e - D_M \omega_m \ , \tag{2}$$

Where H_M is a time constant; T_e is the electromagnetic torque; the damping coefficient $\mathrm{D_M} \approx 0$. When the DFIG is operating in a steady state, $d\omega_m/dt = 0$.

It can be seen from Equations (1) and (2) that the periodic oscillation of T will result in T_e having the same oscillation frequency. Therefore, it can be expressed as:

$$T_e = T_{e0} + T_{ev} \sin(\omega_m t + \varphi) \ , \tag{3}$$

Where T_{e0} and T_{ev} are electromagnetic torques respectively generated by the T_0 and T_v.

What is more, T_e can also be expressed as follows:

$$T_e = \frac{3p}{2} \psi_s i_{sq} \ , \tag{4}$$

978-1-7281-0860-5/19/$31.00 ©2019 IEEE

Where i_{sq} is the q-axis component of i_s; p is the pole pairs; Ψ_s is the stator flux.

What's more[7]:

$$\begin{cases} \dfrac{d\psi_{sd}}{dt} = -R_s i_{sd} + u_{sd} \\ \sigma L_s \dfrac{di_{sd}}{dt} = -\dfrac{L_s R_r + L_r R_s}{L_r} i_{sd} + \dfrac{R_r}{L_r}\psi_{sd} + \\ \qquad \sigma L_s \omega_s i_{sq} + u_{sd} \\ \sigma = 1 - L_m^2 / L_s L_r \end{cases} , \tag{5}$$

Where Ψ_{sd} is the d-axis direction of Ψ_s. i_{sd} is the d-axis direction of i_s. u_{sd} is the d-axis direction of u_s. R_s and L_s are the resistance and inductance of the stator, respectively. R_r and L_r are the resistance and inductance of the rotor, respectively. L_m is the magnetizing inductance and ω_s is the slip angular velocity.

From equation (5), Ψ_{sd} can be obtained in steady-state operation:

$$\psi_{sd} = L_s i_{sd} - \sigma \frac{L_r}{r_r} L_s \omega_s i_{sq} \ . \tag{6}$$

Moreover, the stator flux orientation model indicates that Ψ_{sq}=0. Thus:

$$\psi_s = \psi_{sd} = L_s i_{sd} - \sigma \frac{L_r}{r_r} L_s \omega_s i_{sq} \ , \tag{7}$$

When the DFIG is in a steady state, the stator flux Ψ_s is constant. From Equation (4), it is not difficult to draw:

$$i_{sq} = i_{sq0} + A_{siq} \sin\left(\omega_m t + \varphi_q\right) , \tag{8}$$

Similarly, when combined with Equation (7), i_{sd} should also have the same vibration frequency, as follows:

$$i_{sd} = i_{sd0} + A_{sid} \sin\left(\omega_m t + \varphi_d\right) . \tag{9}$$

The calculated a phase stator current can be calculated as follows with *dq-abc* transformation:

$$\begin{aligned} i_{sa}(t) &= i_0 \sin\left(\omega_e t + \varphi_0\right) + \frac{1}{2}\{A_{sid}\cos[(\omega_e - \omega_m)t - \varphi_d] \\ &+ A_{siq}\cos[(\omega_e - \omega_m)t - \varphi_q]\} \\ &- \frac{1}{2}\{A_{sid}\cos[(\omega_e + \omega_m)t + \varphi_d] \\ &- A_{siq}\cos[(\omega_e + \omega_m)t + \varphi_q]\} \end{aligned} ,\tag{10}$$

where $i_0 = \sqrt{i_{sd0}^2 + i_{sq0}^2}$, $\varphi_0 = \arctan(i_{sq0} / i_{sd0})$, ω_e is the synchronous rotation angular velocity. Usually $\varphi_d \approx \varphi_q$ [7], so:

$$\begin{aligned} i_{sa}(t) &= i_0 \sin(\omega_e t + \varphi_0) + A_1 \cos[(\omega_e - \omega_m)t - \varphi_d] \\ &+ A_2 \cos[(\omega_e + \omega_m)t + \varphi_d] \end{aligned} , \tag{11}$$

where $A_1=(A_{siq}+A_{sid})/2$, $A_2=(A_{siq}-A_{sid})/2$.

The b and c phases can be expressed as:

$$\begin{aligned} i_{sb}(t) &= i_0 \sin(\omega_e t + \varphi_0 - \frac{2\pi}{3}) + A_1 \cos[(\omega_e - \omega_m)t - \varphi_d \\ &- \frac{2\pi}{3}] + A_2 \cos[(\omega_e + \omega_m)t + \varphi_d - \frac{2\pi}{3}] \end{aligned} \tag{12}$$

$$\begin{aligned} i_{sc}(t) &= i_0 \sin(\omega_e t + \varphi_0 + \frac{2\pi}{3}) + A_1 \cos[(\omega_e - \omega_m)t - \varphi_d \\ &+ \frac{2\pi}{3}] + A_2 \cos[(\omega_e + \omega_m)t + \varphi_d + \frac{2\pi}{3}] \end{aligned} \tag{13}$$

Equation (11~13) indicated that the impeller imbalance fault can be diagnosed using the harmonic components with frequency $f_e \pm f_m$($\omega_e=2\pi f_e$, $\omega_m=2\pi f_m$) in the stator current. However, in the early stages of the fault, the fault amplitude of the harmonic component is relatively small. And it is easy to be "submerged" by the basic current. For details, see the corresponding simulation and experimental results.

III. PARK TRANSFORMATION

It can be seen from the above analysis that the impeller imbalance has an effect on the stator current. Using FFT to perform spectral analyzing on the stator current to extract fault characteristics has certain drawbacks, such as harmonic components being easily "flooded". To this end, the Park's Transformation was proposed to process the stator current signal.

The basic idea of Park's Transformation is to convert the three-phase stator current from three-dimensional coordinates to two-dimensional coordinates, especially

$$\begin{cases} i_\alpha = \sqrt{\dfrac{2}{3}} i_a - \dfrac{1}{\sqrt{6}} i_b - \dfrac{1}{\sqrt{6}} i_c \\ i_\beta = \dfrac{1}{\sqrt{2}} i_b - \dfrac{1}{\sqrt{2}} i_c \end{cases} \tag{14}$$

Defining $I(t)=i_\alpha+\mathrm{j}i_\beta$, the square of the stator current Park's Transformation vector is

$$I^2(t) = i_\alpha^2 + i_\beta^2 \tag{15}$$

According to Equations (10)~(15), in the case of impeller imbalance failure, there is

$$\begin{aligned} I^2(t) &= \frac{3}{2}(I_m^2 + I_1^2 + I_h^2) + 3I_m I_1 \cos(\omega_m t - \alpha + \beta) \\ &+ 3I_m I_h \cos(\omega_m t + \alpha - \gamma) + 3I_1 I_h \cos(2\omega_m t + \beta - \gamma) \end{aligned} \tag{16}$$

Equation (15) shows that there are only DC component, 1x axis rotation frequency component and 2x axis rotation frequency component in $I^2(t)$ which can effectively eliminate the interference of the fundamental current. But the amplitude of the 2x-axis rotational frequency component is less than that of the 1x-axis rotational frequency component. So it is only necessary to pay attention to the change of the amplitude of the 1x axis rotation frequency component in $I^2(t)$.

IV. STATOR CURRENT FAULT CHARACTERISTIC EXTRACTION METHOD OF IMPELLER IMBALANCE

The fault diagnosis process of the DFIG impeller imbalance is shown in Figure 1. Specific steps are as follows:

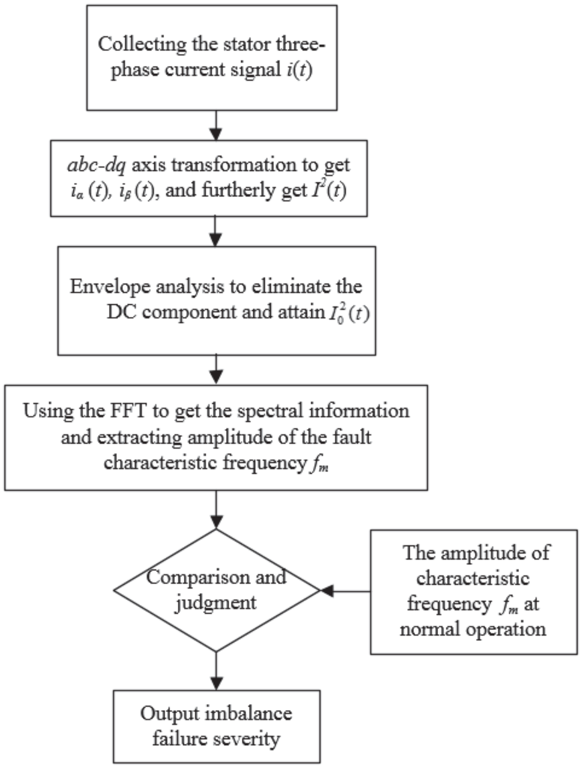

Figure1 Fault diagnosis flowchart

1) Collecting the stator three-phase current $i(t)$ of DFIG and converting $i(t)$ from *abc* three-dimensional coordinates to two-dimensional coordinates by Park's Transformation. And the squared signal $I^2(t)$ can be obtained through Equation (15).

2) Obtaining the upper and lower envelopes of $I_2(t)$ by envelope analysis. Eliminating the DC component by the Equation (17) to obtain $I_0^2(t)$.

$$I_0^2(t) = I^2(t) - [I_{dup}^2(t) + I_{down}^2(t)]/2 \qquad (17)$$

3) By performing spectrum analysis, the amplitude of the fault feature frequency can be obtained. The severity of the impeller imbalance fault can be judged by comparing the feature frequency amplitude in $I_0^2(t)$ with the change in the feature frequency amplitude in normal operation.

V. Simulation Analysis

A. Simulation Model

TABLE I. SIMULATION PARAMETERS

Parameter	Value	Parameter	Value
Rated power (MW)	1.5	Pole pairs	3
Optimum tip-speed ratio	9.94	Stator resistance (Ω)	0.0046
Gearbox speed ratio	90	Stator leakage inductance (H)	0.036
Grid Frequency (Hz)	50	Rotor resistance (Ω)	0.0032
Best wind energy utilization coefficient	0.5	Rotor leakage inductance (H)	0.032
Equivalent inertia time constant (s)	4.32	Magnetizing Inductance (H)	0.575

In order to verify the proposed method, a simulation model of doubly-fed generator with impeller imbalanced fault was constructed. The related parameters are listed in Table 1. To quantify the severity of the impeller imbalance, the impeller imbalance factor F is defined as:

$$F = T_v / T_0 \qquad (18)$$

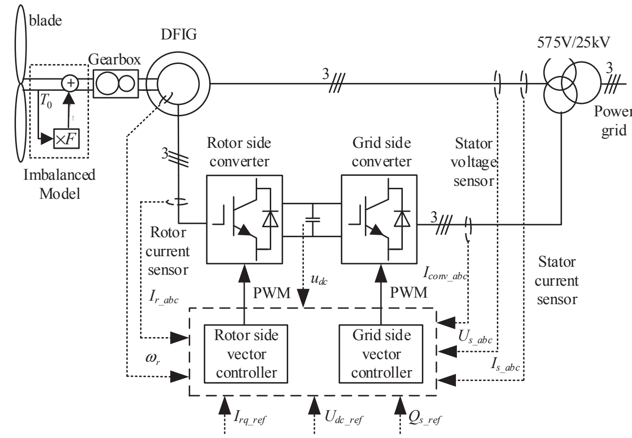

Figure2 Simulation model

B. Different fault characteristics analysis methods Comparison

The proposed method and direct stator phase current spectrum analysis method are compared in this section to verify its effectiveness.

Assuming that the DFIG is operating at a wind speed of 10 m/s (the corresponding impeller rotation frequency is f_m = 0.2 Hz), the DFIG is simulated and studied under normal conditions and F = 6%. In both cases, the time domain and spectral domain waveforms of $I_0^2(t)$ and $i_{sa}(t)$ are shown in Figure 3 when the wind turbine is in a steady state.

Figure 3(a) shows that $I_0^2(t)$ has a regular fluctuation under impeller imbalance in the time domain waveform, while $I_0^2(t)$ remains substantially unchanged under normal conditions. When the impeller is imbalance, $I_0^2(t)$ has a sharp peak at f_m=0.2Hz. In addition, it did not show any protrusions at F = 0%. Therefore, the fault feature can be extracted.

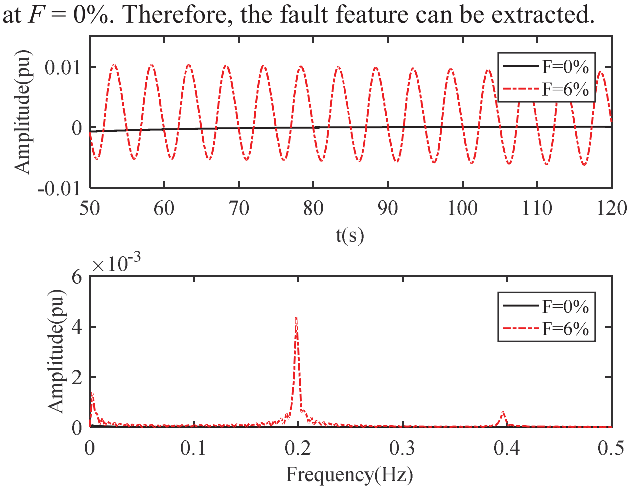

(a) $I_0^2(t)$

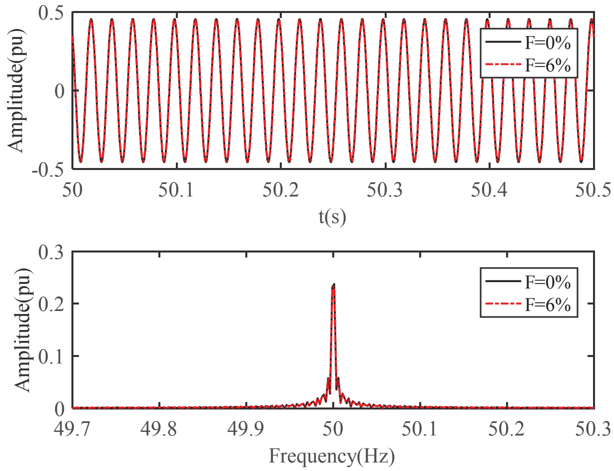

(b) $i_{sa}(t)$

Figure3 Different fault feature analysis methods comparison

Figure 3(b) shows that the time domain waveform of $i_{sa}(t)$ is almost the same in the above two cases. And when the impeller imbalance occurs, the fault feature frequency f_m cannot be effectively distinguished from the frequency domain. Therefore, the fault feature cannot be extracted with this method.

C. *Fault characteristics under unbalanced degrees and different wind speeds*

At 7m/s (f_m=0.125Hz), 10m/s and 13m/s (f_m = 0.22Hz), the DFIG is simulated at F_T = 0%, 2%, 3%, 4%, 5% and 6%. Figure 4 shows the trend of the feature frequency amplitude of $I_0^2(t)$ as the degree of failure increases at different wind speeds.

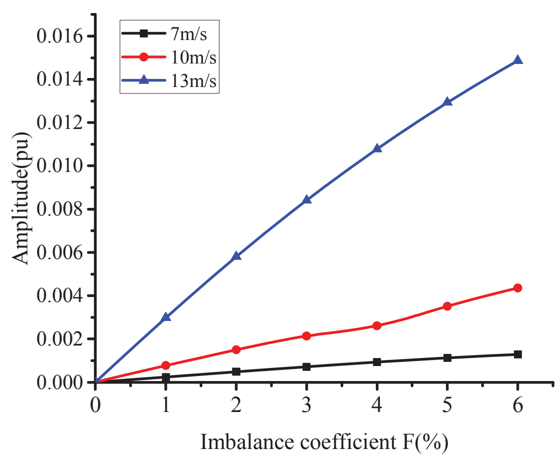

Figure 4 The trend of feature frequency amplitude at different wind speeds

Figure 4 shows that: 1) the larger the wind speed, the larger the feature frequency amplitude of $I_0^2(t)$. The simulation results are consistent with the above theoretical analysis; 2) When F_T = 0%, the amplitude of f_m is mostly equal zero when the wind speed is constant; 3) Operating condition at the same wind speed, the amplitude at f_m changes significantly as the degree of imbalance of the impeller imbalance increases. Therefore, by comparing the change in the feature frequency amplitude of $I_0^2(t)$ with that in normal operation, the severity of the impeller imbalance fault can be determined.

VI. Conclusion

1) The impeller imbalance will cause harmonic components with characteristic frequency $f_e \pm f_m$ in the stator current. However, spectral analyzing on the stator current directly can not effectively extracted the fault feature.

2) When the wind speed is large, the feature frequency amplitude of $I_0^2(t)$ is also large. So, with the proposed fault feature analysis method, the fault severity of the impeller imbalance can be effectively judged through monitoring the feature frequency amplitude variation of $I_0^2(t)$ under the same wind speed condition.

References

[1] C. Christopher J, S Djurovic, P.J. Tavner and A.C. Smith. "Condition monitoring of a wind turbine DFIG by current or power analysis." Iet International Conference on Power Electronics, pp: 311-311, May 2010.

[2] Merabet, Hichem, T. Bahi, and N. Halem. "Condition monitoring and fault detection in wind turbine based on DFIG by the guzzy logic." Energy Procedia. Vol.74, pp: 518-528, Aug 2010.

[3] Jiang Dongxiang, Qian Huang, and Liangyou Hong. "Theoretical and experimental study on wind wheel unbalance for a wind turbine." 2009 World Non-Grid-Connected Wind Power and Energy Conference. IEEE, Qct 2009.

[4] Gardels, Derek J., Wei Qiao, and Xiang Gong. "Simulation studies on imbalance faults of wind turbines." IEEE PES General Meeting. IEEE, Jul 2010.

[5] Caselitz P, Giebhardt J. "Rotor condition monitoring for improved operational safety of offshore wind energy converters". Journal of Solar Energy Engineering, Vol. 127(2), pp:253-261, Apr 2005.

[6] P. A. Joosse, M. J. Blanch, A. G. Dutton, D. A. Kouroussis, T. P. Philippidis and P. S. Vionis. "Acoustic emission monitoring of small wind turbine impellers". Journal of solar energy engineering.Vol. 124.4, pp: 446-454, Nov 2002.

[7] Yang Dong, Ju Tang, and Fuping Zeng. "Impeller imbalance fault diagnosis of doubly fed wind turbine based on current coordinate transformation." IEEJ Transactions on Electrical and Electronic Engineering Vol.14.2 pp: 185-191, Feb 2019.